

V2V Path Loss Modeling at 26 GHz Based on Real-Traffic Measurements

Paweł Kryszkiewicz, Adrian Kliks, *Senior Member, IEEE*, Paweł Sroka, Michał Sybis, *Member, IEEE*

Abstract—In this letter, we investigate single-slope path loss models complemented with shadowing effects in the context of vehicular communications. We present several models obtained based on extensive measurement campaigns with inter-vehicle transmission conducted at 26.555 GHz in real-traffic experiments, mainly along high-speed roads. Particular attention has been put on the impact of aerial characteristics (omnidirectional versus directional), surrounding environment (e.g., urban versus rural), and their mounting point on cars (at the rooftop, on the bumper, and below the car chassis). Finally, the effect of signal ducting and of the number of blocking cars has been analyzed and the decorrelation time has been discussed.

I. INTRODUCTION

RELIABLE wireless vehicle-to-everything (V2X) communications is the basis for secure, intelligent transportation systems of the future [1], [2]. However, various tests have shown that existing communication technologies are sensitive to the wireless channel congestion problem [3]. However, the application of the new frequency bands for V2V purposes entails the need for a precise understanding of signal propagation in typical, everyday scenarios. [4] considers the TV white spaces for data transmission. Complementing it, in [5], we have analyzed the impact of blocking cars on the wireless channel path loss (PL) in the frequency band around 26 GHz.

To model the V2X system operating in sub-30 GHz band correctly and evaluate its performance reliably, the impact of the communication channel on signal propagation has to be precisely analyzed in a dynamic scenario. Various approaches are feasible here for channel modeling, such as those based on ray-tracing/ray-launching, statistical modeling, or utilizing artificial intelligence engine [6]–[8]. While many models can be found for sub-6 GHz bands, there is a limited number of solutions available for higher-frequency scenarios in the V2X context, e.g. in [9]. Moreover, global standardized models could also be mentioned, such as [10] or [11], however, these consider the cellular-specific scenario setup, thus cannot be applied directly for V2V scheme. The 3GPP TR 37.885 model [12] accounts for the specifics of V2V communications in frequencies above 6 GHz, such as low antenna height or

The work has been realized within the project no. 2018/29/B/ST7/01241 funded by the National Science Centre in Poland. The authors are with the Institute of Radiocommunications, Poznan University of Technology, Poznan, Poland, A. Kliks is also with Luleå University of Technology, Luleå, Sweden, email: {pawel.kryszkiewicz, adrian.kliks, pawel.sroka, michal.sybis}@put.poznan.pl. P. Kryszkiewicz is the corresponding author. For the purpose of Open Access, the author has applied a CC-BY public copyright license to any Author Accepted Manuscript (AAM) version arising from this submission.

blockage by other vehicles. However, the split between urban and highway scenarios is available only for the line-of-sight (LOS) case. Moreover, the surrounding environments (such as acoustic shields) are not considered.

The novelty of the paper is the following:

- First, this paper further extends the investigation on the sub-30 GHz channel, focusing on its measurements and modeling for V2V communications in the realtraffic case, including high-speed mode (typically between 50 to 110 kmph) for various configurations. Thus, as a novelty, we present the PL and shadowing models for a real-traffic case, for the 26.555 GHz band using a configuration with communicating antennas located at three different mounting points: on the rooftop, on the cars' bumpers, and below the car.
- Moreover, we conduct the measurements considering: two aerial types - horn and biconical, two environment types - rural and urban, and four surrounding types (in the rural case) - *housing, screens, fields, and forests*.
- We considered three special cases for path loss modeling: the effect of "signal ducting" below the track, blocking cars' impact, and the decorrelation time calculation.
- Finally, let us emphasize that, most importantly, the measurements were performed in a real traffic scenario while driving on a highway near Poznan, Poland. This makes the obtained empirical model highly valuable for practical V2V communications applications.

II. MEASUREMENT SETUP

To conduct the measurements, an extended version of the system setup proposed in [5] has been considered. We have used two cars to carry the needed equipment, as presented in Fig. 1: Citroen C4 Spacetourer being the transmitting vehicle and Peugeot 5008 carrying the receiver. The transmitter has been composed of the Anritsu MG3694A signal generator power-supplied from a portable battery via the power inverter. It has generated a single-carrier signal at the center frequency of 26.555 GHz (a sub-millimeter band, channel n257 of 5G FR2), with the transmit power set to 7 dBm. The chosen transmit power value resulted from the hardware setup's limitations, directional gains of the used antennas, and the radio transmission permit obtained from the Regulator, as we operate in a licensed band. While we used a continuous wave for transmission, the reception bandwidth of 10 kHz used in the spectrum analyzer resulted in a low noise level. This allowed us to measure path loss higher than 130 dB with a distance of up to 1 km, i.e., higher transmit power was not needed.

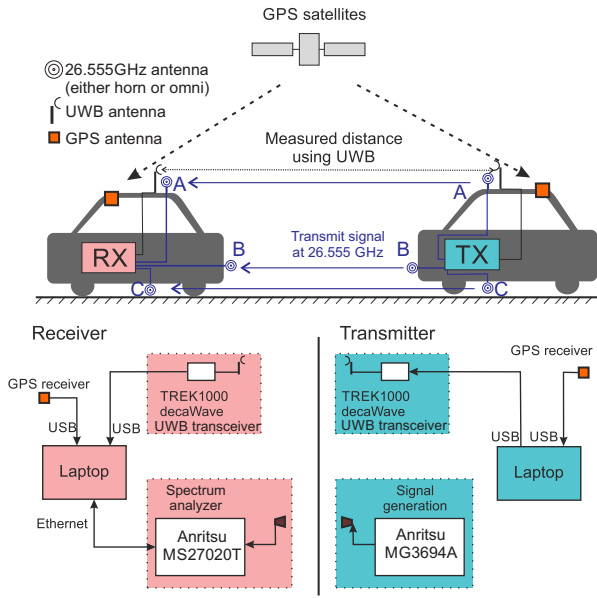


Figure 1. Measurement setup used during the experiment

Signal reception at the receiver has been performed using an Anritsu MS2720T portable spectrum analyzer configured to a Zero Span mode with a Resolution Bandwidth filter of 10 kHz. A single span comprised 551 consecutive power samples obtained over $55ms$. To remove fast fading effects, these samples have been averaged in linear scale to obtain a single, large-scale fading sample. Such a measurement has been executed with a maximum speed of the utilized spectrum analyzer, i.e., approximately every $0.73s$. Such an approach causes the mean value of averaging distance to be within the order suggested by Lee [13], that is, 81.4λ or 10.1λ .

Both the transmitter and the receiver have been connected to antennas using low-loss coaxial cables Jyebao K30K30-53LD-40G150, applying 2.92 mm connectors. Two types of antennas have been considered in this experiment:

- 1) SL-WDPHN-1840-1719-K Skylink directional horn antenna, providing a gain of 19.5 dBi and a half-power angle of about 15 degrees;
- 2) A-info SZ-18004000/P omnidirectional antenna with a gain of about 5 dBi.

We have measured the total attenuation of the used cables to be equal to 18.9 dB at the used frequency. In the specified setup, the maximal path loss that can be estimated is 120.5 dB and 149.5 dB for omnidirectional and directional antennae, respectively. These values were calculated assuming a 1% probability of false alarm (meaning that the noise samples are treated as wanted signals). These values are needed as censoring levels used in the estimation procedure.

The mounting points for the antennas in the vehicles were the following: A. on the rooftop, B. on the rear and the front bumper for the transmitting and receiving vehicle, respectively, C. under the chassis for measuring potential ducting below vehicles. The location of both vehicles and the accurate distance between the transmitter and the receiver have been obtained using both GPS readings and ultra-wideband (UWB) measurements, following the rationale explained

in [14]. GPS measurements are characterized by up to a few meters inaccuracy. This becomes significant when short inter-vehicle distances are considered. The UWB measurement is much more accurate but available only for a limited range. Therefore, we have applied a combination of both methods, following [14], with TREK1000 devices used to process the UWB signal.

During the measurement experiment the cars forming the platoon drove along the route presented in Fig. 2. It had begun in front of the premises of Poznan University of Technology in Poznan, Poland, with the measurements carried out across the Poznan city center and suburbs. The total length of this section was approximately 12 km. Then, after leaving the urban area, the experiment was continued along the high-speed road until the intermediate point near Kornik city had been reached. Finally, the route followed along the rural road for over 13 km. Next, the measurements were carried out on the highway section between two junctions; the platoon was driving in both directions back and forth, reaching a total travel distance of 25 km. We followed various parts of the route a couple of times, changing the antennas' mounting points and their type.



Figure 2. The measurement route chosen for the drive campaigns

III. PATH LOSS MODELS

A. Prerequisites

The ultimate goal of the conducted experiments was to identify the impact of various environmental factors on the propagation measured by means of the proposed path loss model. First, following the approach proposed in [15] and also employed in our previous work [16], we tried to distinguish the line-of-sight (LOS) and non-LOS (NLOS) propagation. To achieve this goal, the whole experiment has been recorded from the receiving car, and the video has been carefully analyzed with a millisecond precision by post-processing it frame-by-frame.

Moreover, the samples have been precisely tagged to indicate various environmental factors and scenarios. First, all LOS and NLOS samples have been classified as "Urban" or "Rural," where the former reflects the measurements carried inside the city, and the latter - those collected outside the city. Second, we used marks: *fields*, *screens*, *forest* and *housing* to reflect the impact of the surrounding environment. In detail, *fields* represent the scenario with the field

areas (with no houses, bigger infrastructure, forests, or bigger bushes). *Screens* illustrate the case where acoustic shields were mounted at least on one side of the street (and the environment behind them does not matter). *Forest* represents the case when the road went through the forestry areas, and *housing* - where houses were around. A sample was tagged as described above when the receiving car entered a certain area. Please note that some classes might be overlapping, what has to be taken into account while analyzing the results. To minimize the impact of transition, the samples collected around the transition time have been discarded.

Please note that we have repeated our measurements, as we tried to collect as many samples as necessary to guarantee the statistical correctness of the channel modeling process. However, as the experiments have been carried out in real-life scenarios, situations occurred where the total number of samples (which could be tagged as presented above) or their distance variability was not satisfactory. Thus, we do not present PL models in such cases, marking them as unavailable.

B. Modelling Process

Our focus is to propose a simple model that will be easily applicable in various real-life V2V scenarios where exact knowledge about the details of the environment cannot be easily acquired (to go for, e.g., ray-tracing-based solutions). Thus, from the variety of options, we selected the single-slope approach, which is widely used in different contexts. As proposed in [17], the path loss and shadowing were estimated using Maximal Likelihood estimators. We applied the single-slope path loss model operating in the logarithmic scale for distance d , complemented with the log-normal shadowing component, as presented below:

$$L(d) = A \log_{10} \left(\frac{d}{10} \right) + B + N(0, C), \quad (1)$$

where $A \log_{10} \left(\frac{d}{10} \right)$ represents the impact of increased distance, referring to the distance of 10 m, B defines the bias observed at the reference distance of 10 m, and the last component $N(0, C)$ corresponds to the impact of shadowing, modeled using a normal distribution with 0 mean and standard deviation C . Please note that the reference distance was chosen to allow for easy comparison of path loss at 10 m between different models by looking at B parameters, yet it can be easily transformed into any other needed value. The rationale behind the selection of 10 m was the following: such a distance may frequently appear in an urban scenario. Moreover, it can be treated as the minimum (possibly unsafe) distance between cars, e.g., while overtaking or in a platooning scenario. The selected AB model offered us the necessary level of flexibility while keeping complexity at a very low level, as compared to, e.g., CI or log-distance models, where such flexibility was slightly reduced [18]. Please note that the path loss depends mainly on the distance (explicitly provided in the model), and the frequency (included inside the B parameter), as the measurements have been done for a single frequency, representative for the FR2 band. Should the other frequencies be measured, the frequency-dependent component could be included as well, e.g., $20 \log_{10}(f)$.

In Fig. 3 an example of the ML path loss model fitting is shown. One may observe here two models (marked as *urban* and *rural*) for each of the two considered variants (LOS and NLOS). In the LOS case, both urban and rural PL are very similar, so the environment does not have that strong impact when there is a direct link available - we observe nearly free-space propagation, as the A coefficient is close to 20. Next, comparing the LOS and NLOS cases, we see a more substantial shadowing impact in the latter case, which is compliant with typical models specified in, e.g., 3GPP documents [11]. Finally, in the NLOS case, we observe a higher impact of the scattering elements around vehicles in the urban case.

C. Discussion on Results

Our measurements have considered two kinds of antennas: omnidirectional and directional. While we considered maximal antennas' gain (similarly as utilized cables attenuation) removing it from the measurements, we did not include the directivity gain of the antenna, i.e., an additional attenuation that is introduced by both TX and RX antennas not facing each other with the maximal directivity directions. The obtained path loss models include potential penalty introduced by this effect in a real traffic scenario.

Three antennas' mounting points have been investigated: on the rooftop, on the bumper, and under the chassis. The comparative results for the first two mounting locations are presented in Tab. I. Let us remember that the table consists of two parts: the left compares the PL models for urban and rural environments, whereas the right part illustrates the impact of the surrounding items in the environment (*fields, screens, forest, housing*).

Various conclusions could be drawn here by comparing the presented models. First, one may observe interesting differences in the obtained models between the mounting point for the omnidirectional antennas. As the PL models are relatively similar for the LOS case, they are quite different for the NLOS variant. For example, it is particularly visible when one compares the results for the NLOS channel in an Urban environment, where there is almost a difference of

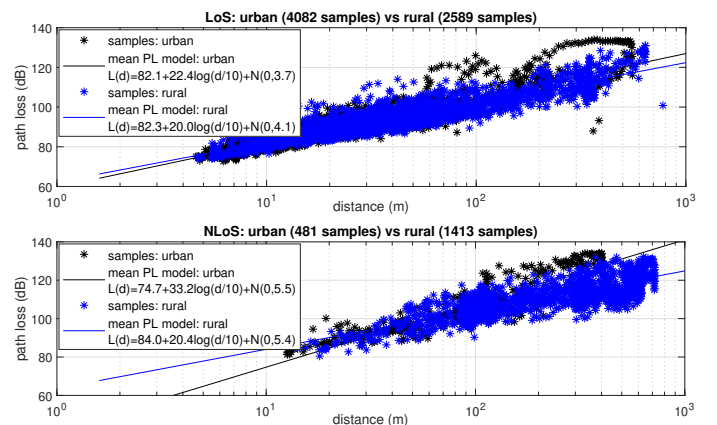


Figure 3. Measurements and modeling results for omni-antenna mounted on the roof; lines in the figure do not contain the shadowing component.

Table I. comparison of the path loss coefficients for various experimentation variants

	Path loss format $L(d) = A \log_{10} \left(\frac{d}{10} \right) + B + N(0, C)$; Presentation form {A,B,C}						
	Channel	Urban	Rural	Fields	Screens	Forest	Housing
Omnidirectional at the rooftop	LOS	{22.4, 82.1, 3.7}	{20.0, 82.3, 4.1}	{19.4, 82.6, 3.9}	{23.1, 79.9, 5.3}	{17.6, 83.8, 3.9}	{22.9, 82.1, 3.6}
	NLOS	{33.2, 74.7, 5.5}	{20.4, 84.0, 5.4}	{20.5, 84.7, 5.0}	{21.7, 80.4, 4.6}	{21.2, 82.7, 6.0}	{35.2, 72.4, 5.8}
Omnidirectional at the bumper	LOS	{25.1, 79.9, 5.2}	{19.4, 84.9, 5.9}	{24.6, 80.6, 5.3}	{19.6, 81.7, 3.8}	{-, -, -}	{29.9, 80.3, 3.8}
	NLOS	{14.5, 93.0, 4.1}	{18.6, 87.7, 4.9}	{14.5, 92.9, 4.6}	{28.0, 76.5, 4.0}	{-, -, -}	{-, -, -}
Directional at the rooftop	LOS	{15.0, 80.6, 8.9}	{13.9, 86.4, 7.8}	{11.8, 86.8, 9.2}	{15.5, 84.0, 3.7}	{11.7, 88.6, 4.5}	{13.8, 80.4, 9.2}
	NLOS	{-, -, -}	{16.9, 90.1, 6.4}	{20.1, 87.4, 6.8}	{24.4, 77.7, 4.9}	{-, -, -}	{-, -, -}
Directional at the bumper	LOS	{-, -, -}	{5.2, 94.1, 9.1}	{16.2, 93.5, 6.4}	{-, -, -}	{-, -, -}	{-, -, -}
	NLOS	{-, -, -}	{16.2, 93.5, 6.4}	{17.3, 92.4, 6.2}	{-, -, -}	{-, -, -}	{-, -, -}

20 between A and B values (33.2, 74.7, 5.5 for the rooftop and 14.5, 93.0, 4.1 for the bumper). It means that when the antenna is mounted on the bumper, the signal suffers from significant constant attenuation introduced by the intermediate cars (obstacle-car causing NLOS), and the impact of the distance is not that severe. It is the opposite for the rooftop mounting point, where the impact of the blocking car is much smaller, and the signal attenuates more steeply with distance.

Next, one can compare the PL models for LOS and NLOS for rural areas when the omnidirectional antenna is mounted on the rooftop; they are very similar; thus, it could be reasonable to combine them into one model and not distinguish between the LOS and NLOS cases. Similarly, for the same mounting point of the omni-antenna and NLOS channel, the differences between the PL models achieved for non-housing surroundings are again relatively small.

In general, for omni-antenna mounted on a rooftop, one can see the significant impact of the environment, especially when comparing *urban* versus *rural*, or *housing* and *screens* versus *fields* and *forests*. This impact is particularly noticeable in the NLOS case. With *screens* or *housing* as well as in the *urban* scenarios, the change in attenuation of the signal with distance is much stronger (A is around 20) than in *rural*, *fields* and *forest* cases (A is above 30).

An interesting phenomenon can be observed when analyzing a variant with a directional antenna on the rooftop, and comparing the measurement results with those for an omni-antenna. First, in some cases, the shadowing component is very high (maximally even above 9 dB).

Second, the impact of the first, distance-related component A , is weaker. For omni-antenna, it takes values around 20, while for directional antennas - between 11 and 16. At the same time, the bias values B are comparable in both cases.

Various conclusions can be drawn based on the achieved results; however, due to the limited space, we decided to highlight the last observation. For the directional antenna located on the bumper, the bias coefficient B is very high (above 93 dB), in both cases, where we were able to collect a reasonable number of samples (i.e. for *rural* and *fields*). In general, changing the location from the roof to the bumper increases B coefficient.

IV. HIGHLIGHTS ON SPECIFIC ASPECTS

A. Antennas Mounted Below the Car

The intention of mounting antennas below the cars was to investigate the potential of wave ducting in the tunnel between the street pavement and bottoms of the vehicles (especially trucks), as the clearance is potentially relatively ample. The following PL models have been achieved for LOS:

- for urban area: $L(d) = 36.9 \cdot \log \left(\frac{d}{10} \right) + 91.7 + N(0, 3.3)$;
- rural area $L(d) = 22.1 \cdot \log \left(\frac{d}{10} \right) + 95.3 + N(0, 3.4)$.

One can notice the high values of bias B (above 90 dB), and, at the same time, the high impact of distance on PL - A is above 22 for rural and close to 37 for urban areas. Moreover, the shadowing variance is relatively small. Achieved results show that under-the-car communication faces very strong signal attenuation if the antennas are too close to the car chassis. Furthermore, we have evaluated the impact of the surrounding elements on signal propagation. We achieved reliable measurements for two variants:

- for *fields* $L(d) = 23.9 \cdot \log \left(\frac{d}{10} \right) + 94.1 + N(0, 3.8)$;
- for *screens* $L(d) = 20.9 \cdot \log \left(\frac{d}{10} \right) + 94.5 + N(0, 3.7)$.

B. Impact of Number of Cars on the Path Loss

Finally, we attempted to check if there is a significant change in PL observed when the number of blocking cars changes. In the dynamic, real-life experiment, we collected a reliable number of samples for the case where either omni-directional or horn antennas were mounted on bumpers and when there were one (Case A) or more cars (i.e., more than one, (Case B) between the transmitter and the receiver. The results are summarized below:

- Omni, Case A $L(d) = 12.5 \cdot \log \left(\frac{d}{10} \right) + 92.8 + N(0, 4.1)$;
- Omni, Case B $L(d) = 12.0 \cdot \log \left(\frac{d}{10} \right) + 94.8 + N(0, 3.9)$;
- Horn, Case A $L(d) = 1.5 \cdot \log \left(\frac{d}{10} \right) + 104.3 + N(0, 5.1)$;
- Horn, Case B $L(d) = 6.9 \cdot \log \left(\frac{d}{10} \right) + 106.5 + N(0, 5.6)$.

The results are interesting, as there is no evident difference between the cases with one or more than one blocking cars. The dominating factor is the location of the aerial. In the case of the horn antenna, one may observe the almost negligible impact of the distance ($A = 1.5$ for one blocking car), whereas the bias is very high - above 100 dB. For multi-car case, the coefficient A increases to 6.9. Let us stress that the measurements were collected for distances from 30 to 50 m for Case A and from 100 to 200 for Case B, which specifies the validity range of the proposed models.

C. Comparison with 3GPP TR37.885

We compared our results with one of the popular models defined in [12]. As the model considers various cases, here we put results for the LoS highway ($PL = 32.4 + 20 \log_{10}(d_{3D}) + 20 \log_{10}(f_c)$) and NLoS ($PL = 36.85 + 30 \log_{10}(d_{3D}) + 18.9 \log_{10}(f_c)$) channel, for which the environment specification and the mathematical model specification (single-slope model) is similar to the one used in our paper. Fixing $f_c = 26.555$ GHz, the TR 37.885 model results for LoS case in: $A = 20.0, B = 80.88, C = 3$, and for NLoS case in: $A = 30.0, B = 93.77, C = 4$. Comparing these results with those in Tab. I, one can observe relatively high similarity between these two models. Visibly, the TR 37.885 LoS model is very close to our model for the omnidirectional antenna mounted on the rooftop: comparing the B parameter, the path loss difference is lower than 1.5 dB at a 10 m distance. As in both 3GPP and our proposal $A = 20$, the path loss difference will not increase for other distances. However, as different antenna mounting points impact path loss, the TR 37.885 model diverges more for the other antennas and mounting points analyzed in this paper. Our model is more specific.

D. Decorrelation Time

Finally, we have processed the collected samples to verify what is the decorrelation time T_d of the channel shadowing using Gudmundson model [19], i.e., the time when the normalized autocorrelation achieves $\frac{1}{e}$ value. Calculation details are described in [16]. Achieved results depend on the antenna mounting point, receiver velocity V_{RX} and relative velocity between the transmitter and the receiver V_{TX-RX} (both velocities are quantized). The results are placed in Tab. II. When the RX car does not move, T_d is high (above 14 s). However, when cars are moving, T_d is much smaller. This shows that even if inter-vehicle communications is blocked at some time instance by high shadowing, after a few seconds, the shadowing will be uncorrelated, possibly allowing for transmission; higher T_d is observed for the rooftop mounting point.

Table II. Decorrelation time [s]

	$V_{TX-RX} \left[\frac{m}{s} \right]$	0	2	4
Omnidirectional at the rooftop	$V_{RX} = 0 \left[\frac{m}{s} \right]$	14.57	-	22.44
	$V_{RX} = 10 \left[\frac{m}{s} \right]$	1.09	1.00	4.91
	$V_{RX} = 20 \left[\frac{m}{s} \right]$	1.66	2.64	9.04
Omnidirectional at the bumper	$V_{RX} = 0 \left[\frac{m}{s} \right]$	128.02	-	-
	$V_{RX} = 10 \left[\frac{m}{s} \right]$	1.41	2.21	5.34
	$V_{RX} = 20 \left[\frac{m}{s} \right]$	4.40	4.37	3.07

V. CONCLUSIONS

In this paper, we presented the set of various single-slope PL models for V2V mmWave propagation generated based on rich measurement campaigns conducted in a real-traffic environment. We identified that it is hard to identify some generic trends on how the mounting point influences the resultant observed PL. One may observe that the bias (B component) increases in NLOS scenario when the antenna is located on the rooftop, on the bumper, and below the car.

However, besides that, the overall impact is noticeable, yet the generic rules are hard to specify. Second, the potential ducting effect below the car chassis requires further analysis, as the placement of antennas on a 15 cm arm does not guarantee reliable communications. Third, there are reasonable differences in PL in urban and rural cases; however, the distinction between various surrounding elements is justified if particularly needed. Fourth, the impact of blocking cars - well reflected in static scenarios - is not that well visible in the case of antennas mounted on the bumper when cars are moving. Finally, the correlation time is around of a couple of seconds in the full mobility scenario.

REFERENCES

- [1] Y. Zheng, S. Eben Li, J. Wang, D. Cao, and K. Li, "Stability and scalability of homogeneous vehicular platoon: Study on the influence of information flow topologies," *IEEE Transactions on Intelligent Transportation Systems*, vol. 17, no. 1, pp. 14–26, 2016.
- [2] S. Ucar, S. C. Ergen, and O. Ozkasap, "IEEE 802.11p and Visible Light Hybrid Communication Based Secure Autonomous Platoon," *IEEE Trans. on Vehicular Technology*, vol. 67, no. 9, pp. 8667–8681, 2018.
- [3] V. Vukadinovic *et al.*, "3GPP C-V2X and IEEE 802.11p for Vehicle-to-Vehicle communications in highway platooning scenarios," *Ad Hoc Networks*, vol. 74, pp. 17 – 29, 2018.
- [4] P. Sroka, A. Kliks, M. Sybis, and P. Kryszkiewicz, "Dynamic Power and Frequency Allocation Scheme for Autonomous Platooning," in *IEEE 93rd Vehicular Technology Conf. (VTC2021-Spring)*, pp. 1–6, 2021.
- [5] P. Kryszkiewicz, A. Kliks, P. Sroka, and M. Sybis, "The Impact of Blocking Cars on Pathloss Within a Platoon: Measurements for 26 GHz Band," in *International Conference on Software, Telecommunications and Computer Networks (SoftCOM)*, pp. 1–6, 2021.
- [6] I. A. Hemadeh, K. Satyanarayana, M. El-Hajjar, and L. Hanzo, "Millimeter-wave communications: Physical channel models, design considerations, antenna constructions, and link-budget," *IEEE Communications Surveys Tutorials*, vol. 20, no. 2, pp. 870–913, 2018.
- [7] C. Wang, J. Bian, J. Sun, W. Zhang, and M. Zhang, "A Survey of 5G Channel Measurements and Models," *IEEE Communications Surveys Tutorials*, vol. 20, no. 4, pp. 3142–3168, 2018.
- [8] K. Zheng, L. Zhao, J. Mei, B. Shao, W. Xiang, and L. Hanzo, "Survey of large-scale mimo systems," *IEEE Communications Surveys Tutorials*, vol. 17, no. 3, pp. 1738–1760, 2015.
- [9] J. Huang, C. X. Wang, H. Chang, J. Sun, and X. Gao, "Multi-Frequency Multi-Scenario Millimeter Wave MIMO Channel Measurements and Modeling for B5G Wireless Communication Systems," *IEEE Journal on Sel. Areas in Comm.*, vol. 38, no. 9, pp. 2010–2025, 2020.
- [10] "Report ITU-R M.2412-0; Guidelines for evaluation of radio interface technologies for IMT-2020," 2017.
- [11] "3GPP TR 38.901, Study on channel model for frequencies from 0.5 to 100 GHz;(release 16), v16.1.0," 2020.
- [12] "3GPP TR 37.885, Study on evaluation methodology of new Vehicle-to-Everything (v2x) use cases for LTE and NR;(rel. 15), v15.3.0," 2019.
- [13] D. de la Vega *et al.*, "Generalization of the Lee Method for the Analysis of the Signal Variability," *IEEE Transactions on Vehicular Technology*, vol. 58, no. 2, pp. 506–516, 2009.
- [14] P. Kryszkiewicz, M. Sybis, P. Sroka, and A. Kliks, "Distance Estimation for Database-assisted Autonomous Platooning," in *15th EAI CROWN-COM*, pp. 1–6, 2020.
- [15] M. Boban, J. Barros, and O. K. Tonguz, "Geometry-based vehicle-to-vehicle channel modeling for large-scale simulation," *IEEE Transactions on Vehicular Technology*, vol. 63, no. 9, pp. 4146–4164, 2014.
- [16] P. Kryszkiewicz, P. Sroka, M. Sybis, and A. Kliks, "Path Loss and Shadowing Modeling for Vehicle-to-Vehicle Communications in Terrestrial TV Band," *IEEE Trans. on Antennas and Propagation*, vol. 71, no. 1, pp. 984–998, 2023.
- [17] C. Gustafson, T. Abbas, D. Bolin, and F. Tufvesson, "Statistical modeling and estimation of censored pathloss data," *IEEE Wireless Communications Letters*, vol. 4, no. 5, pp. 569–572, 2015.
- [18] S. Sun *et al.*, "Propagation Path Loss Models for 5G Urban Micro- and Macro-Cellular Scenarios," in *IEEE 83rd Vehicular Technology Conference (VTC Spring)*, pp. 1–6, 2016.
- [19] M. Gudmundson, "Correlation model for shadow fading in mobile radio systems," *Electronics Letters*, vol. 27, pp. 2145–2146(1), Nov. 1991.